Development 124, 1941-1952 (1997)
Printed in Great Britain © The Company of Biologists Limited 1997
DEV8416

Competition and cooperation among receptor tyrosine phosphatases control motoneuron growth cone guidance in *Drosophila*

Chand J. Desai[1], Neil X. Krueger[2], Haruo Saito[2] and Kai Zinn[1,*]

[1]Division of Biology, California Institute of Technology, Pasadena, California 91125, USA
[2]Division of Tumor Immunology, Dana-Farber Cancer Institute and Department of Biological Chemistry and Molecular Pharmacology, Harvard Medical School, Boston, Massachusetts 02115, USA

*Author for correspondence (e-mail: zinnk@starbase1.caltech.edu)

SUMMARY

The neural receptor tyrosine phosphatases DPTP69D, DPTP99A and DLAR are involved in motor axon guidance in the *Drosophila* embryo. Here we analyze the requirements for these three phosphatases in growth cone guidance decisions along the ISN and SNb motor pathways. Any one of the three suffices for the progression of ISN pioneer growth cones beyond their first intermediate target in the dorsal muscle field. DLAR or DPTP69D can facilitate outgrowth beyond a second intermediate target, and DLAR is uniquely required for formation of a normal terminal arbor. A different pattern of partial redundancy among the three phosphatases is observed for the SNb pathway. Any one of the three suffices to allow SNb axons to leave the common ISN pathway at the exit junction. When DLAR is not expressed, however, SNb axons sometimes bypass their ventrolateral muscle targets after leaving the common pathway, instead growing out as a separate bundle adjacent to the ISN. This abnormal guidance decision can be completely suppressed by also removing DPTP99A, suggesting that DLAR turns off or counteracts a DPTP99A signal that favors the bypass axon trajectory. Our results show that the relationships among the tyrosine phosphatases are complex and dependent on cellular context. At growth cone choice points along one nerve, two phosphatases cooperate, while along another nerve these same phosphatases can act in opposition to one another.

Key words: receptor tyrosine phosphatase, growth cone, *Drosophila*, neuromuscular system, neural development, neurogenetics

INTRODUCTION

During nervous system development, neuronal growth cones are directed toward their synaptic targets by interactions with cell-surface and secreted molecules (reviewed by Goodman, 1996). Such interactions can produce cytoskeletal rearrangements in the growth cone that steer it in the appropriate directions (Fan and Raper, 1995; reviewed by Bentley and O'Connor, 1994).

One mechanism linking growth cone behavior to contact with guidance cues is the control of phosphotyrosine signaling via direct or indirect activation of tyrosine kinases. Activation of Eph receptor tyrosine kinases (RTKs) can cause growth cone collapse and regulate axon fasciculation in tissue culture systems, and interactions between Eph kinases and their cell-surface ligands may be important in establishing connections between the retina and optic tectum (reviewed by Harris and Holt, 1995). Mutations in mouse Eph kinase genes affect formation of commissural axon pathways in the brain (Henkemeyer et al., 1996; Orioli et al., 1996). The nonreceptor tyrosine kinases Src and Fyn are required for stimulation of neurite outgrowth by the cell adhesion molecules L1 and N-CAM, and their expression patterns suggest that these kinases could also be involved in pathfinding in vivo (Beggs et al., 1994; Ignelzi et al., 1994). In *Drosophila*, the Drl RTK is expressed on a subset of central nervous system (CNS) neurons, and the axons of these neurons make incorrect pathway choices in *drl* mutant embryos (Callahan et al., 1995).

Receptor tyrosine phosphatases (RPTPs), which reverse reactions catalyzed by tyrosine kinases, are expressed on neuronal processes in *Drosophila* (reviewed by Chien, 1996) and vertebrates (Stoker et al., 1995). RPTPs often have extracellular domains homologous to those of neural adhesion molecules and are implicated in the regulation of adhesion in neurons and epithelial cells (reviewed by Fashena and Zinn, 1995). The RPTP LAR, a vertebrate ortholog of *Drosophila* DLAR, localizes to focal adhesions and binds to a guanine nucleotide exchange factor for the small GTPases Rac and Rho (Debant et al., 1996; Serrapages et al., 1995). These GTPases, together with the related molecule Cdc42, control cytoskeletal rearrangements that are important for cell movement and growth cone guidance processes (reviewed by Chant and Stowers, 1995).

The neural RPTPs DPTP69D, DPTP99A, and DLAR are required for motor axon guidance during the development of the *Drosophila* embryonic neuromuscular system. Mutations in the *Ptp69D* and *Dlar* genes produce distinct, partially penetrant motor axon guidance phenotypes, while *Ptp99A* mutations are

silent except in a *Ptp69D* mutant background (Desai et al., 1996; Krueger et al., 1996). To further explore the roles of DPTP69D, DPTP99A and DLAR in growth cone guidance, we have examined the motor axon phenotypes of embryos bearing combinations of mutations in all three genes. This analysis reveals that a hierarchy of RPTPs controls navigation of growth cones along one pathway. At a specific choice point along another pathway, two RPTPs act in opposition to one another to control a guidance decision.

MATERIALS AND METHODS

The mutant lines used in this study were described previously (Desai et al., 1996; Hamilton et al., 1995; Krueger et al., 1996). The genes previously called *dptp69D* and *dptp99A* have been renamed *Ptp69D* and *Ptp99A*, respectively, to conform to current Flybase nomenclature. Flybase refers to *Dlar* as *Lar.* We retain the name *Dlar* in this paper, however, to avoid confusion with vertebrate LAR. *Df(3R)KE* was provided by W. Chia. Anti-Twist antiserum was from S. Roth. Embryo collections and immunohistochemistry were done as described by Desai et al. (1996). As in this study, we identified *Ptp69D* and *Ptp99A* mutants by the absence of staining with monoclonal antibodies (mAbs) against DPTP69D and DPTP99A. Non-staining embryos were sorted, restained with mAb 1D4, and dissected. There is no available antibody against DLAR, so we used a *CyOlacZ* balancer and stained embryos with anti-β-galactosidase mAb (Promega) to identify *Dlar* embryos. Double-balanced stocks (*Dlar/CyOlacZ, Ptp69D/TM3 or TM6BlacZ*) containing both *Dlar* and *Ptp69D* mutations could not be generated and sorted embryos (from crosses involving *Dlar/CyOlacZ, Ptp69D Ptp99A/+* genotypes) that had been stained with antibodies against β-galactosidase, DPTP69D, and DPTP99A often exhibited poor 1D4 staining. Thus, for some of the *Dlar* mutant combinations we initially defined diagnostic phenotypes (not those being scored) by examining *Dlar* embryos identified with the *lacZ* balancer as described above, but used crosses with *Dlar/+* genotypes in order to score phenotypic penetrance in subsequent collections. Embryos from such crosses were stained with anti-DPTP69D and/or anti-DPTP99A mAbs, and non-staining embryos were stained with mAb 1D4, dissected and sorted for *Dlar* genotype using diagnostic axonal phenotypes. The DPTP69D transgene used for overexpression were described previously (Desai et al., 1996); multiple copies of the transgene were crossed into *Dlar* backgrounds.

Figures were made by scanning negatives and creating Photoshop 3.0.5 files. Figs 1, 2, and 4 (most panels), and Fig. 6B are montages created by merging images of slightly different focal planes. The use of montages allows visualization of the entire pathway of a nerve in a single image. The nerves usually traverse different focal planes, making it difficult to capture an entire nerve in one photograph.

RESULTS

DPTP69D, DPTP99A and DLAR are selectively expressed on CNS axons in stage 12-17 embryos (reviewed by Chien, 1996). DPTP69D and DPTP99A can be visualized on motor axons and growth cones (Desai et al., 1996). DLAR is detectable on the nerve roots in which motor axons exit the CNS (Tian et al., 1991), but anti-DLAR antisera are insufficiently sensitive to allow visualization of the protein on the smaller peripheral motor nerves. DLAR mRNA is expressed by many CNS neurons, including the identified RP motoneurons (Krueger et al., 1996; Tian et al., 1991). Neither DPTP69D and DPTP99A proteins nor DLAR mRNA are detectably expressed by embryonic muscle cells (Desai et al., 1996; Krueger et al., 1996).

Because embryonic neuromuscular junctions are highly stereotyped and easily visualized, their development provides an excellent system in which to examine pathfinding by CNS growth cones. Approximately 40 motoneurons innervate 30 identified muscle fibers in each abdominal hemisegment (A2-A7) of the embryo. Axons from these neurons exit the CNS via the segmental nerve (SN) and intersegmental nerve (ISN) roots and then extend within five nerve pathways. SNa and SNc emerge from the SN root, while SNb, SNd and the ISN arise from the ISN root (reviewed by Keshishian et al., 1996). All of these nerves can be visualized using a single mAb, 1D4, which recognizes the cytoplasmic domain of the cell-surface protein Fasciclin II (Van Vactor et al., 1993).

To accurately assess the motor axon phenotypes of *Rptp* mutants, we analyzed embryos bearing different combinations of alleles at each locus. These alleles were placed over each other or over independently generated deficiency mutations to eliminate potential effects of mutant chromosomes being homozygous. For *Ptp69D*, we primarily used two nonoverlapping deletions, $Ptp69D^{1}$ and *Df(3L)8ex25*, derived by excision of different *P*-elements. $Ptp69D^{1}$ removes DNA encoding most of the extracellular domain including the signal sequence. *Df(3L)8ex25* deletes most or all of the DNA encoding the cytoplasmic domain, but is not a null allele. We also examined $Ptp69D^{1}$ over *Df(3L)8ex34*, which deletes the entire gene, as well as *Df(3L)8ex25* over *Df(3L)8ex34* (Desai et al., 1996). For *Ptp99A*, we used *Df(3R)R3* over either $Ptp99A^{1}$ or *Df(3R)KE*. Only 5-10 kb of DNA are deleted in $Ptp99A^{1}$/*Df(3R)R3* flies, all of which is within the *Ptp99A* gene (Hamilton et al., 1995). *Df(3R)KE/Df(3R)R3* flies lack essentially all DPTP99A coding sequences. Both genotypes are viable and fertile. The mutations $Dlar^{5.5}$ and $Dlar^{13.2}$ are EMS alleles that introduce termination codons into the DLAR extracellular domain. These point mutations were usually examined over each other or over a small (100 kbp) deficiency, *Df(2L)OD16*, which removes almost all DLAR coding sequence. We also examined the phenotypes of mutant combinations involving *Df(2L)E55*, which removes genes 5′ to *Dlar* and the first three small exons of *Dlar* (Krueger et al., 1996).

Intersegmental nerve development in wild-type embryos

The growth cone of the aCC neuron pioneers the ISN pathway, exiting the CNS during stage 13 and then growing dorsally past the ventrolateral muscles (VLMs) and lateral muscle 4 (Figs 1A, 3A). During stage 15, ISN growth cones contact one of the three dorsal ‘persistent Twist’ (PT) cells, PT2 (Fig. 1B,C), and also interact with the peripheral nervous system (PNS) and muscle fibers. The PT cells are precursors of adult muscles (Bate et al., 1991) and express both Twist (a mesodermal nuclear marker) and Fasciclin II.

Another PT cell, PT3, is initially located posterior and lateral to PT2 and does not appear to be contacted by the pioneer axons during their outgrowth (Fig. 1B). Later, however, PT3 is contacted by a posteriorly directed side branch of the ISN (Fig. 1C), and it subsequently migrates toward the main nerve (Fig. 1D-F). After passing PT2, the pioneer growth cones extend under the main tracheal trunk and contact a third PT cell, PT1,

as well as the muscle fibers adjacent to it (Van Vactor et al., 1993; Fig. 1E,F).

By the end of stage 16, the ISN has acquired a highly stereotyped morphology, with lateral branches at the proximal edges of muscles 3 (first branch) and 2 (second branch) and a terminal arbor at the proximal edge of muscle 1, just beyond PT1 (Figs 2A, 3A). PT3 is always at the first branchpoint (Figs 1F, 2A). ISN axons form synapses on the dorsal muscles during stage 16 and early stage 17, with aCC innervating muscle 1 and RP2 innervating muscle 2 (Sink and Whitington, 1991).

Mutant combinations involving *Dlar* produce specific intersegmental nerve truncation phenotypes

In wild-type, *Ptp99A*, or *Ptp69D* late stage 16 embryos, the ISN has reached PT1 and begun to form a terminal arbor in 99-100% of abdominal hemisegments (A2-A7) (Table 1). *Dlar* embryos, however, display truncation phenotypes in which 9-19% of ISNs terminate at the second lateral branchpoint (SB phenotype; Fig. 3B), and 22-34% stop between the second branch and PT1 (SB+ phenotype; Table 1). The distal portion of the ISN is often abnormally thin in SB+ hemisegments, suggesting that some axons failed to extend past the second branchpoint (Fig. 2B). ISNs that do reach PT1 usually form terminal arbors that are smaller and simpler than in wild-type, suggesting that growth cone exploration of the muscle fibers near PT1 is reduced in *Dlar* mutants (Fig. 2B).

Combining *Ptp69D* with *Dlar* increases the penetrance and severity of the *Dlar* ISN defects. In *Dlar, Ptp69D* double mutant embryos, only 15-19% of ISNs reach PT1, while 43-49% stop at the position of the second branchpoint (Figs 2C, 3B). *Dlar, Ptp99A* double mutants also display SB (10-21%) and SB+ (29-39%) phenotypes (Table 1). About 5% of ISNs terminate at the first branchpoint in both types of double mutants, a phenotype not observed in any single mutant embryo. *Ptp69D Ptp99A* embryos occasionally have abnormal ISNs, but much less frequently than in the other double mutant genotypes (5% SB, 11% SB+; Table 1).

Triple mutants lacking all three RPTPs exhibit much stronger ISN phenotypes than any single or double mutant. 57-70% of ISNs now terminate at the first lateral branchpoint near PT3 (FB phenotype; Figs 2D, 3C), while 12-17% of ISNs fail to even reach PT3 (1- phenotype; Table 1, see also Fig. 4F).

Truncation phenotypes would result if the pioneer ISN growth cones in *Rptp* mutants failed to extend beyond intermediate targets during their outgrowth. Short ISNs could also result from extension beyond intermediate targets followed by retraction. Our data do not favor retraction, because we do not observe an increased frequency of longer ISNs in multiply mutant embryos at earlier stages (data not shown).

The *Rptp* mutant phenotypes described here suggest that intermediate targets for ISN growth cones may be located at the two branchpoint positions where ISN truncations are observed. The first branchpoint position is at the intersection between muscle 19 and the proximal edge of muscle 3 (Figs 2A,D, 3A). The second branchpoint position is at the intersection of the proximal edges of muscles 10 and 2 (Figs 2A,C, 3A). There may also be a target site at the intersection of the proximal edges of muscles 1 and 9 that defines the position of the terminal arbor. PT1 is also located here (Figs 1F, 2A, 3A; see Bate, 1993 for a review of the muscle pattern).

Although processes branching from the ISN later envelop it (Fig. 2A), PT3 does not appear to be directly contacted by the pioneer growth cones (Fig. 1B,C), so it is unlikely to define an intermediate target for the main ISN. PT2 is dorsal to the first branchpoint by stage 16 (Figs 1E,F, 2A). ISN pioneer growth cones reproducibly contact PT2, however, and the first lateral branch forms shortly after this contact is made (Fig. 1B,C), so

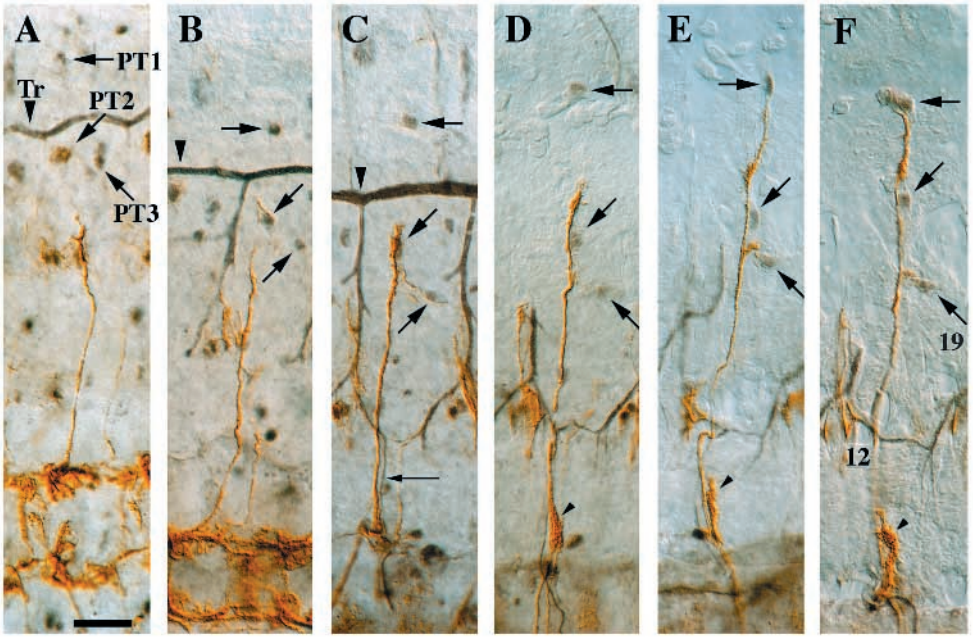

Fig. 1. Timeline of wild-type ISN development. Stage 14 to early stage 16 embryos were stained with anti-Twist antiserum (black) and mAb 1D4 (brown). PT1, PT2 and PT3 are indicated by horizontal arrows, downward arrows, and upward arrows, respectively. Anti-Twist also fortuitously stains tracheal branches, allowing visualization of the relationship between nerves and tracheae. The main tracheal trunk is indicated by large arrowheads in A-C, but was dissected away in D-F. The increasing distance between the CNS and PT1 from A to F is due to expansion of the epidermis during dorsal closure. (A) The pioneer growth cones of the ISN have passed the VLMs and the lateral PT cells but have not yet reached PT2. (B,C) The growth cones contact and envelop PT2, and the side branch to PT3 forms. Note that the ISN grows under the VLMs before the ventral tracheal branch (thin arrow) develops. (D) The ISN growth cones are between PT2 and PT1. SNb growth cones (small arrowheads in D-F) are at the exit junction. (E) The ISN contacts PT1. A separate SNb branch is visible. (F) Muscle differentiation is now evident (muscles 12 and 19 are indicated). Anterior is to the left. Scale bar, 4 μm.

recognition of PT2 could be involved in defining the first branchpoint position.

In summary, our results show that all three RPTPs are involved in ISN outgrowth and guidance. In *Dlar* single mutants, most ISNs reach PT1 but have small terminal arbors (Fig. 2B). ISNs with any abnormal phenotype are uncommon (<17% penetrance) in any single or double mutant genotype in which *Dlar* is wild-type, suggesting that DLAR is central to ISN guidance. Removing *Ptp69D* and/or *Ptp99A* function from *Dlar* mutants generates phenotypes in which the ISN pathway is truncated at specific branchpoint positions. Thus, while DPTP69D or DPTP99A are not essential for ISN development, they do participate in guidance processes involving DLAR. These results are graphically displayed for a matched set of single, double and triple mutant genotypes in Fig. 3D-G.

To investigate the basis of the requirement for DLAR, we examined the ISN phenotypes of *Dlar* embryos in which DPTP69D is overexpressed. The frequency of the SB truncation phenotype in these embryos (10%) was similar to that observed in *Dlar* embryos (Table 1), and they still had small terminal arbors (data not shown). These data suggest that DPTP69D cannot substitute effectively for DLAR along the ISN pathway even when it is present at much higher than normal levels (see Desai et al., 1996 for a description of DPTP69D overexpression).

DPTP69D and DLAR are required for SNb pathfinding and synaptogenesis within the ventrolateral muscle field

The SNb motor nerve innervates the ventrolateral muscles (VLMs) and contains the axons of the identified RP1, RP3, RP4 and RP5 motoneurons. RP growth cones leave the common ISN pathway at the exit junction (EJ), enter the VLM field, and then navigate among the muscle fibers (reviewed by Keshishian et al., 1996). Synapses form at highly stereotyped positions by late stage 16 (Figs 4A, 5A-B, 6A).

Previous results demonstrated that loss of *Ptp69D* function produces SNb phenotypes in which the nerve follows abnormal pathways among the muscle fibers or stalls prior to reaching synaptic targets. Although *Ptp99A* mutations on their own cause no SNb phenotypes, removal of DPTP69D uncovers a role for DPTP99A in SNb axon guidance. SNb axons in *Ptp69D* single mutants and *Ptp69D Ptp99A* double mutants display similar guidance defects (Fig. 4B,C). The penetrance of these defects, however, is increased about 7-fold by removal of *Ptp99A* function (Desai et al., 1996; Table 2).

Here we show that *Dlar* mutations also affect SNb guidance and synaptogenesis within the VLM field. In 62-74% of hemisegments in *Dlar*-null embryos, the entire SNb navigates the exit junction and successfully enters the VLMs (Table 2). Most of these SNbs fail to form the normal pattern of synaptic branches. The morphologies of the abnormal SNbs in *Dlar* mutants, however, are quite different from those in *Ptp69D Ptp99A* mutants. *Dlar* SNbs in late stage 16/early stage 17 embryos have the overall appearance of wild-type SNbs at early to mid-stage 16, suggesting that their development is delayed. They are thick and terminate in large growth cones at the distal edge of muscle 6. The prominent synapse in the cleft between muscles 7 and 6 is usually absent, as is the synapse at muscle 12 (Figs 4D, 6C).

Dlar mutations produce SNb navigation errors at the muscle field entry point

Navigation errors at two or more choice points can produce

Table 1. ISN phenotypes in *Rptp* mutant embryos

		Phenotype (%)				
Genotype	*n*	T	SB+	SB	FB	1-
Ptp69D						
Ptp69D^{1}/Df(3L)8ex25	131	99	1	0	0	0
Ptp69D Ptp99A						
Ptp69D^{1} Df(3R)R3/Df(3L)8ex25 Ptp99A^{1}	172	83	11	5	0	1
Dlar						
Dlar$^{5.5}$/Dlar$^{13.2}$	256	59	22	19	0	0
Dlar$^{5.5}$/Df(2L)OD16	141	68	23	9	0	0
Dlar$^{13.2}$/Df(2L)OD16	240	54	34	12	0	0
*Dlar$^{13.2}$/Df(2L)E55**	479	73	18	14	1	0
Dlar Ptp69D						
Dlar$^{5.5}$/Dlar$^{13.2}$; Ptp69D^{1}/Df(3L)8ex25	287	19	27	49	5	0
Dlar$^{5.5}$/Df(2L)OD16, Ptp69D^{1}/Df(3L)8ex34	213	15	37	43	4	0
Dlar Ptp99A						
Dlar$^{5.5}$/Dlar$^{13.2}$; Df(3R)R3/Ptp99A^{1}	215	35	39	21	5	0
Dlar$^{5.5}$/Df(2L)OD16, Df(3R)R3/Df(3R)KE	83	60	29	10	1	0
Dlar Ptp69D Ptp99A						
Dlar$^{5.5}$/Dlar$^{13.2}$; Ptp69D^{1} Df(3R)R3/Df(3L)8ex25 Ptp99A^{1}	172	1	3	23	62	12
Dlar$^{5.5}$/Dlar$^{13.2}$; Ptp69D^{1} Ptp99A^{1}/Df(3L)8ex25 Ptp99A^{1}	96	1	1	13	70	16
Dlar$^{5.5}$/Df(2L)OD16; Ptp69D^{1} Ptp99A^{1}/Df(3L)8ex25 Ptp99A^{1}	60	0	2	25	57	17
***Dlar* plus extra DPTP69D**						
P[69D4-2.11]/+ or >; Dlar$^{13.2}$/Df(2L)OD16; P[69D3-1.17]	238	78	12	10	0	0

n=Number of hemisegments (A2-A7) scored. T: ISNs that appear to reach the terminal arbor position at PT1; note that terminal arbors are smaller than normal in most *Dlar* hemisegments. SB+: ISNs that are thinner than normal between the second branchpoint and the terminus or that extend past the second branchpoint but fail to reach PT1. SB: ISNs that terminate at the second branchpoint. FB: ISNs that terminate at the first branchpoint. 1-: ISNs that terminate proximal to the first branchpoint. The numbers listed are % of hemisegments displaying a particular phenotype.

*Embryos laid by *Df(2L)E55* mothers had phenotypes that were not significantly different from those laid by *Dlar$^{13.2}$* mothers, so the two sets of embryos were combined for this entry.

phenotypes in which SNb axons fail to enter the VLM field and the muscles remain uninnervated (see diagrams in Fig. 5A-D). The 'fusion bypass' (F) phenotype is observed when SNb axons completely fail to defasciculate from the common ISN pathway at the exit junction (Figs 4F,G, 5D, 6D). This phenotype was previously described in *Ptp69D Ptp99A* mutants (Desai et al., 1996). In fusion bypass hemisegments, SNb axons continue to extend distally within the ISN tract and fail to innervate the VLMs.

SNb axons can also leave the common ISN pathway at the exit junction in an apparently normal manner, but then fail to enter the VLM field. This produces the 'parallel bypass' phenotypes seen in *Dlar* mutants (Krueger et al., 1996), in which SNb axons grow underneath the VLMs as a separate tract adjacent to the ISN (Figs 4D,E, 5C, 6B). Although fusion bypass and parallel bypass both result in a lack of VLM innervation, they are distinct phenotypes produced by navigation errors at the exit junction and VLM entry point, respectively.

In complete parallel bypass (P) hemisegments (17-19% in *Dlar*-nulls), all SNb axons follow the abnormal pathway, while in partial parallel bypass (PP) hemisegments (8-12%), some SNb axons enter the VLMs and others bypass them (Table 2). To further study the roles of DLAR and DPTP69D in controlling guidance decisions at the VLM entry point, we analyzed the phenotypes of double mutants and examined whether overexpressed DPTP69D could replace DLAR. In *Dlar*-null embryos, 26-38% of hemisegments display partial or complete parallel bypass phenotypes. When *Ptp69D* function is also removed, a larger percentage (46-59%) now have these phenotypes. Conversely, overexpressing DPTP69D in a *Dlar* background produces a small decrease in bypass penetrance (to 16%; Table 2). These results indicate that although parallel bypass is not observed unless DLAR is absent, DLAR and DPTP69D may have overlapping functions in controlling the probability that SNb growth cones will make an abnormal decision at the VLM entry point.

All three RPTPs regulate defasciculation of SNb axons at the exit junction

Some axons do enter the VLM field in 58-69% of *Dlar*; *Ptp69D* hemisegments, indicating that SNb growth cones can follow guidance cues at the exit junction and VLM entry point in the absence of both RPTPs. To determine whether such growth cones still use RPTP signaling for pathfinding, we examined SNbs in triple mutant embryos that also lack DPTP99A. In these triple mutants, only 4-7% of hemisegments have any axons that enter the VLMs (Table 2).

SNb axons in triple mutants display two kinds of phenotypes. One of these is fusion bypass (Figs 4F,G, 6D), in

Table 2. SNb phenotypes in *Rptp* mutant embryos

		Phenotype (%)*			
Genotype	*n*	PP	P	S	F
Ptp69D					
Ptp69D^{1}/Df(3L)8ex25	141	2	0	1	0
Ptp69D Ptp99A					
Ptp69D^{1} Df(3R)R3/Df(3L)8ex25 Ptp99A^{1}†	192	2	1	14	4
Dlar					
Dlar$^{5.5}$/Dlar$^{13.2}$‡	260	12	19	4	3
Dlar$^{5.5}$/Df(2L)OD16	143	8	17	0	1
Dlar$^{13.2}$/Df(2L)OD16	132	10	17	11	0
Dlar Ptp69D					
Dlar$^{5.5}$/Dlar$^{13.2}$; Ptp69D^{1}/Df(3L)8ex25	288	30	16	12	3
Dlar$^{5.5}$/Df(2L)OD16; Ptp69D^{1}/Df(3L)8ex34‡	216	28	31	9	2
Dlar Ptp99A					
Dlar$^{5.5}$/Dlar$^{13.2}$; Df(3R)R3/Ptp99A^{1}	214	1	0	3	0
Dlar$^{5.5}$/Df(2L)OD16; Df(3R)R3/Df(3R)KE	84	1	1	8	0
Dlar$^{5.5}$/Df(2L)OD16; Ptp99A^{1}/Ptp99A^{1}	130	4	0	7	1
Dlar Ptp69D Ptp99A					
Dlar$^{5.5}$/Dlar$^{13.2}$; Ptp69D^{1} Df(3R)R3/Df(3L)8ex25 Ptp99A^{1}	167	1	1	59	36
Dlar$^{5.5}$/Dlar$^{13.2}$; Ptp69D^{1} Ptp99A^{1}/Df(3L)8ex25 Ptp99A^{1}	90	1	1	37	55
Dlar$^{5.5}$/Df(2L)OD16, *Ptp69D^{1} Ptp99A^{1}/Df(3L)8ex25 Ptp99A^{1}*	60	0	0	33	61
***Dlar* plus extra DPTP69D**					
P[69D4-2.11]; Dlar$^{13.2}$/Df(2L)OD16, P[69D3-1.17]	235	7	9	3	0

n=Number of hemisegments (A2-A7) scored. PP: partial parallel bypass, in which some SNb axons bypass the VLM field and grow out adjacent to the ISN. P: complete parallel bypass, in which all SNb axons bypass the VLMs and grow out adjacent to the ISN. S: SNbs that stall prior to entering the VLMs. F: fusion bypass, in which SNb axons never leave the ISN pathway and bypass the VLMs in the ISN tract.

*The numbers are % of hemisegments exhibiting a specific phenotype. The percentages do not add up to 100 in this table, because we have not included columns for SNbs that enter the VLMs. Note that SNbs that do enter the VLMs are not necessarily wild-type. For example, in *Dlar* and *Ptp69D Ptp99A* mutants most SNbs have abnormal morphologies, as described in the text.

†The penetrance of the F phenotype (4%) in this genotype is very low relative to that previously reported (Desai et al., 1996) for *Ptp69D^{1} Ptp99A^{1}* homozygotes (about 50%). In general, we observe that while heterozygous genotypes still display a high overall percentage of abnormal SNbs, the frequency of F or S phenotypes is lower than in double mutants homozygous for *Ptp69D^{1}*. This could be due to a closely linked phenotypic enhancer on the *Ptp69D^{1}* chromosome or to a recessive antimorphic phenotype caused by a truncated DPTP69D protein that might be made from this chromosome. We have examined double and triple mutant embryos bearing the *Ptp69D* genotype *Df(3L)8ex25/Df(3L)8ex34*, and find that these have similar phenotypes to the corresponding *Ptp69D^{1}/Df(3L)8ex25* embryos, indicating that *Ptp69D^{1}* does not confer a dominant phenotype (data not shown).

‡The frequency of the P phenotype is twofold greater for the genotype bearing the total deletion *Df(3L)8ex34* than for that bearing the hypomorphic *Df(3L)8ex25*. Most other phenotypic frequencies are similar for the two genotypes (see Table 1).

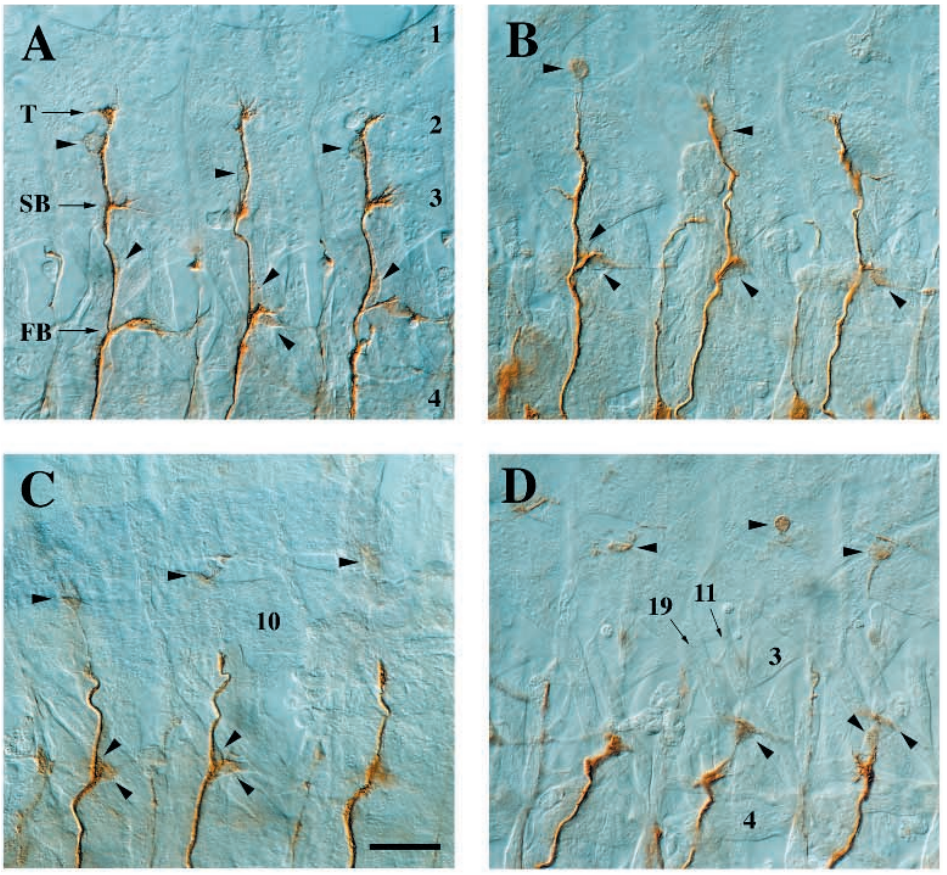

Fig. 2. ISN phenotypes in *Rptp* mutant embryos. Each panel shows the dorsal region of three abdominal hemisegments in late stage 16 embryos stained with mAb 1D4 (brown). Muscles are labeled with numbers and PT cells are indicated (horizontal, downward, and upward arrowheads as in Fig. 1) in some hemisegments. (A) Wild-type pattern. Note the stereotyped positions of the first (FB) and second (SB) lateral branches, and the terminal arbor (T). PT3 is crossed by the first branch and is between muscles 11 and 19. (B) *Dlar* pattern, showing small terminal arbors and thinning of distal ISN in left hemisegment. (C) SB phenotype (ISN termination at the second branchpoint position), in a *Dlar Ptp69D* embryo. Note the stereotyped position of the termini of the truncated ISNs at the proximal edge of muscle 10. (D) FB phenotype (ISN termination at the first branchpoint position), in a triple mutant. The terminus of each truncated ISN is between muscles 11 and 19, near the proximal edge of muscle 3. Anterior is to the left. Scale bar, 5 μm.

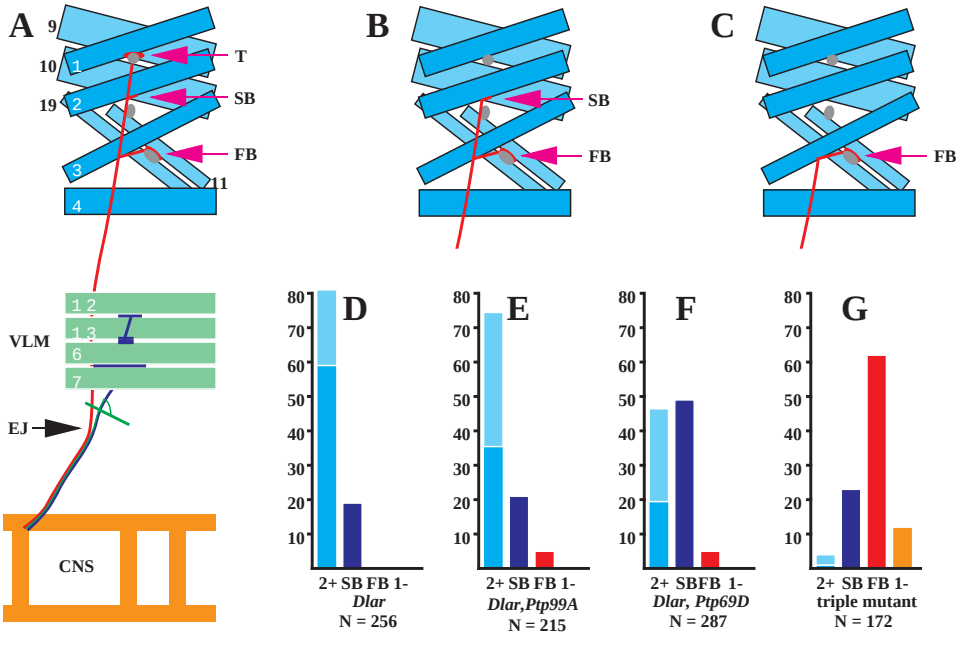

Fig. 3. Schematic diagrams and bar graphs of ISN phenotypes. Some of the dorsal and lateral muscles are depicted in A-C (blue rectangles), as are the PT cells (grey), and the ISN (red). The first (FB) and second (SB) lateral ISN branch positions and the terminal arbor (T) are indicated. (A) Wild-type, showing relative positions of the ISN, SNb (blue) and SNd (green) nerves, the exit junction (EJ), the dorsal and ventrolateral (VLM, green rectangles) muscles, and the CNS axon array (orange). (B) SB truncation, characteristic of *Dlar, Ptp69D*. (C) FB truncation, characteristic of triple mutant. The ordinates of the bar graphs in (D-G) represent the penetrances (in %) of the various phenotypes. Blue bars represent ISNs that reach the terminal arbor position at PT1. These arbors are usually smaller than normal in *Dlar* mutants. Light blue bars represent ISNs that are thinner than normal between SB and the terminal arbor position, suggesting that some ISN axons failed to reach the terminus (denoted as SB+ in the text). These categories are combined here into one column, which is labeled as 2+ (meaning that these ISNs extend past SB). SB: ISN termination at the second branchpoint (purple bars). FB: ISN termination at the first branchpoint (red bars). 1-: ISN stops proximal to FB (orange bars). N=number of hemisegments scored. (D) $Dlar^{5.5}/Dlar^{13.2}$. (E) $Dlar^{5.5}/Dlar^{13.2}$; $Df(3R)R3/Ptp99A^{1}$. (F) $Dlar^{5.5}/Dlar^{13.2}$; $Ptp69D^{1}/Df(3L)8ex25$. (G), $Dlar^{5.5}/Dlar^{13.2}$; $Ptp69D^{1}Df(3R)R3/Df(3L)8ex25\ Ptp99A^{1}$.

which the axons never defasciculate from the common ISN pathway. 36-61% of hemisegments have fusion bypass phenotypes in triple mutants, while less than 4% of hemisegments display such phenotypes in any double mutant combination (Table 2, Fig. 5E-J). The other SNb phenotype frequently observed in triple mutants (33-59%) is the 'complete stall' (S). In complete stall hemisegments, the SNb leaves the common ISN pathway but does not reach the VLM entry point, instead growing posteriorly for a short distance and then stopping (Fig. 4F,G). Since essentially all SNb axons in triple mutants display F or S phenotypes, it cannot be determined whether P phenotypes, which involve navigation errors at a later choice point, could also exist in these genotypes.

The complete stall and fusion bypass phenotypes might both be caused by an inability of SNb axons to defasciculate. After leaving the ISN at the exit junction, SNb and SNd axons normally follow a short shared pathway that splits at a nearby second junction (see Fig. 5A for diagram). If SNb axons successfully navigated the exit junction but then failed to leave the shared SNb/SNd pathway and the abnormal combined pathway stopped growing, this could produce the club-like SNb morphology characteristic of the complete stall. It was previously shown that 70% of *Dlar* hemisegments lack SNds (Krueger et al., 1996). We find that distinct SNd branches are never observed in hemisegments displaying complete stall phenotypes, consistent with the hypothesis that the stalled SNbs also contain SNd axons.

In summary, our results show that the three RPTPs have overlapping and partially redundant activities in controlling defasciculation of SNb axons. Fusion bypass is seldom observed in any genotype in which *Ptp69D* is wild-type, suggesting that DPTP69D is central to the defasciculation decision at the exit junction. Removal of DPTP99A (from

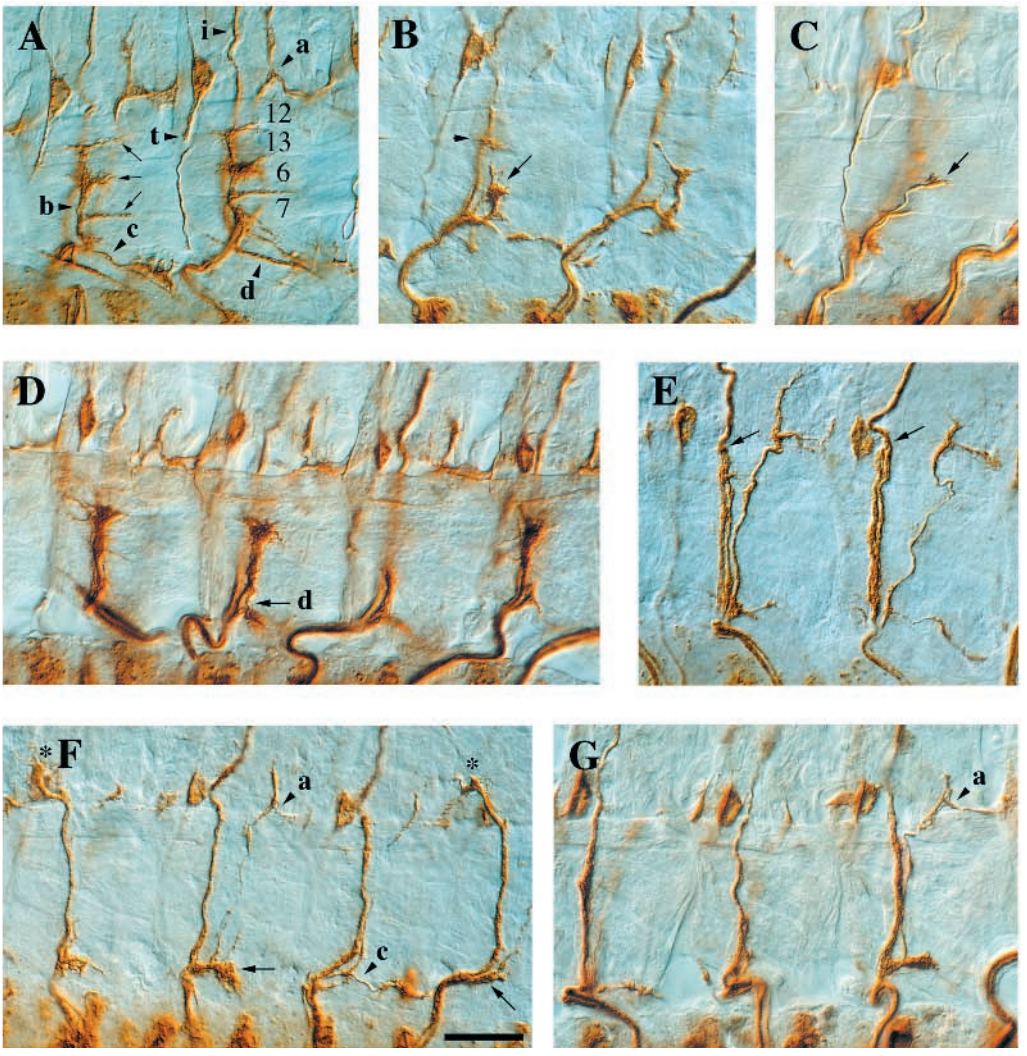

Fig. 4. SNb phenotypes in *Rptp* mutant embryos. Each panel shows abdominal hemisegments in late stage 16/early stage 17 embryos stained with mAb 1D4 (brown). Some of the ventrolateral muscles are numbered in A. (A) Wild-type. The transverse nerve (t), ISN (i), SNa (a), SNb (b), SNc (c), and SNd (d) are labeled. Note the stereotyped synaptic branches at the muscle 12/13 cleft (upper arrow), under muscle 6 (middle arrow), and at the muscle 6/7 cleft (lower arrow). (B) *Ptp69D Ptp99A*. The left SNb split. Some axons entered the VLM field normally but stalled on muscle 7 (arrow) and extended a short branch. Other axons remained fasciculated with the ISN until they grew beneath muscle 13. There they defasciculated from the ISN, entered the VLM field at an abnomal site, and then formed synapses at a normal target, along the base of muscle 13 (arrowhead). (C) *Ptp69D Ptp99A*. SNb axons grew on the wrong (interior) side of the VLMs in this hemisegment. Note the apparent innervation of the muscle 6/7 cleft from the wrong side (arrow; focal plane is at interior face of the VLMs). The remainder of the SNb is out of focus underneath the VLMs. (D) *Dlar*. Hemisegments 1 (left), 2, and 4 display the 'immature SNb' phenotype within the VLMs. Note that the SNbs are very thick and have not formed synapses, although this is an embryo at approximately the same stage as the one in A. Hemisegment 3 has a parallel bypass phenotype. Only one hemisegment has an SNd nerve (arrow). In E-G, deep focal planes are shown, so that the ISN, bypass SNbs, and SNas can be visualized. (E) *Dlar, Ptp69D*; parallel bypass phenotypes. Note the parallel tracts in each hemisegment. The SNb appears to rejoin the ISN near the distal edge of the VLMs (arrows). (F) Fusion bypass and complete stall phenotypes, in a triple mutant. Hemisegments 2 and 4 have complete stall phenotypes (arrows), while hemisegment 3 has a fusion bypass phenotype. In hemisegments 1 and 4, the combined ISN/SNb pathways stall near the proximal edge of muscle 4, just distal to the VLMs (*; denoted as 1- phenotype in Fig. 3). Note the normal SNa bifurcation (arrowhead) and the SNc branch (thin arrow). (G) Fusion bypass, in a triple mutant. Note the thick but completely fused ISN tracts in hemisegments 1 and 3 (compare to E). Anterior is to the left. Scale bar, 5 μm.

Dlar, Ptp69D) or DLAR (from *Ptp69D Ptp99A*) to generate the triple mutant produces a 10- to 20-fold increase in the frequency of fusion bypass (compare Fig. 5H with G and I; Table 2). The frequency of complete stall phenotypes is also increased by >4-fold. All of these data are graphically summarized for a matched set of single, double and triple mutant genotypes in Fig. 5E-J.

Ptp99A mutations suppress the *Dlar* parallel bypass phenotype

The *Dlar* parallel bypass phenotype results from a failure of SNb axons to enter the VLM field after defasciculating from the ISN and forming a separate pathway. Strikingly, we find that when three different *Ptp99A* genotypes are introduced into a *Dlar* background, the complete parallel bypass phenotype is suppressed, from 17-19% in *Dlar*-nulls to <1% in *Dlar, Ptp99A* (Table 2; Figs 5E,F, 6B,C). Partial parallel bypass phenotypes are also greatly reduced, from 8-12% to 1-4%. Suppression is specific for parallel bypass decisions, because *Ptp99A* mutations have little or no effect on the failure of *Dlar* SNbs to form synapses within the VLM field (Fig. 6C), or on the frequency of stall phenotypes. Note that *Dlar* single mutants occasionally display phenotypes that we scored as fusion bypass (1-3%), and such phenotypes are also not seen in *Dlar Ptp99A* double mutants (Table 2; Fig. 5E,F). This may indicate that these apparent fusion bypass SNbs actually did defasciculate from the common pathway at the exit junction, but then grew out in a tract so close to the ISN that it could not be resolved as a separate bundle by light microscopy.

These results suggest that the decision made by SNb axons in *Dlar* mutants to grow alongside the ISN rather than entering the VLM field is likely to be due to inappropriately active DPTP99A rather than to a failure of DLAR-mediated VLM recognition. One function of DLAR may be to negatively regulate or counteract PTP99A signaling at the VLM entry point.

Interactions of *Ptp99A* with the extreme *Dlar* allele *Df(2L)E55*

The penetrance of the complete parallel bypass phenotype (17-19%; Table 2) that we observed in *Dlar*-null embryos ($Dlar^{5.5}/Dlar^{13.2}$, $Dlar^{5.5}/Df(2L)OD16$, and $Dlar^{13.2}/Df(2L)OD16$) is much lower than that previously reported (>60%) for these *Dlar* point mutations over *Df(2L)E55* (Krueger et al., 1996). Here we show that this greater penetrance seen in *Df(2L)E55* genotypes involves both maternal and zygotic contributions. When *Df(2L)E55/CyO* males are crossed with $Dlar^{13.2}/CyO$ females, the resulting *Dlar* embryos exhibit a 31% penetrance of complete parallel bypass. When *Df(2L)E55/CyO* females are crossed with $Dlar^{13.2}/CyO$ males, however, a penetrance of 63% is observed (Table 3). We do not yet understand why *Df(2L)E55*, which deletes the promoter region and the first three small exons of *Dlar*, increases SNb bypass penetrance beyond the levels observed in a *Dlar*-null. Two possibilities are: (1) a truncated *Dlar* protein could be made from the *Df(2L)E55* chromosome, and this protein might be made at the wrong time or have an ectopic activity that increases parallel bypass penetrance; (2) removal of one copy of another gene located under *Df(2L)E55* may produce an enhancement of the bypass phenotype. The penetrances of the ISN and SNd defects are similar in all *Dlar* genotypes (Table 1; Krueger et al., 1996), so the effects of *Df(2L)E55* appear to be specific to the SNb bypass phenotype.

Since the parallel bypass phenotype in *Dlar*-nulls appears to be completely dependent on *Ptp99A* function, we investigated whether this is also true of the enhanced phenotypes of *Df(2L)E55* combinations. Our results show that DPTP99A is also essential for these phenotypes, because removal of both maternal and zygotic *Ptp99A* function from *Df(2L)E55* genotypes reduces the penetrance of parallel bypass to 4%. Removal of only maternal or only zygotic DPTP99A produces intermediate penetrances (10-11%; Table 3). In contrast, the results described above (Table 2; Fig. 5E,F) show that removal of only zygotic DPTP99A is sufficient to completely suppress parallel bypass in *Dlar*-null genotypes. Fig. 6 shows the various SNb phenotypes in multiple segments of embryos lacking one, two, or three of the RPTPs, and illustrates the striking effects of removal of DPTP99A in a *Dlar* background.

Effects of *Rptp* mutants on other axon pathways

The ISN, SNb and SNd motor nerves that branch from the ISN root are particularly sensitive to loss of RPTP activity. By contrast, the SNa and SNc motor nerves, which branch from

Table 3. SNb phenotypes in *Df(2L)E55/Dlar* single and double mutant embryos

Genotype	*n*	Phenotype (%) PP	P	S	F
Dlar					
$Df(2L)E55/Dlar^{13.2}$ (males were *E55*)*	479	14	31	1	1
$Df(2L)E55/Dlar^{13.2}$ (females were *E55*)†	240	10	63	0	0
Dlar Ptp99A					
$Df(2L)E55/Dlar^{13.2}$; $Ptp99A^{1}/Df(3R)R3$ (no maternal DPTP99A)‡	239	4	4	0	0
$Df(2L)E55/Dlar^{5.5}$; $Ptp99A^{1}/Df(3R)R3$ (females were *Ptp99A*/+)§	240	8	10	1	0
$Df(2L)E55/Dlar^{13.2}$; *Ptp99A*/+ (no maternal DPTP99A)¶	264	8	11	1	0

n=Number of hemisegments (A2-A7) scored. Phenotypes are as defined in the legend to Table 2. As in Table 2, the percentages do not add up to 100, because we have not included columns for SNbs that enter the VLMs.

*w; $Dlar^{13.2}/CyOlacZ$ females were crossed to *Df(2L)E55/CyOlacZ* males.

†*Df(2L)E55/CyOlacZ* females were crossed to w; $Dlar^{13.2}/CyOlacZ$ males.

‡w; $Dlar^{13.2}/CyO$; $Ptp99A^{1}/Df(3R)R3$ females were crossed to $Df(2L)E55/+$, $Ptp99A^{1}/+$ males, and *Ptp99A* progeny were selected by antibody staining.

§The *Ptp99A* embryos from crosses of w; *Df(2L)E55*/+; *Df(3R)R3*/+ males × w; $Dlar^{5.5}/+$; $Ptp99A^{1}/+$ females and w; $Dlar^{5.5}/+$; $Ptp99A^{1}/+$ males × w/+; *Df(2L)E55*/+; *Df(3R)R3*/+ females were pooled.

¶w; $Dlar^{13.2}/CyO$; $Ptp99A^{1}/Df(3R)R3$ females were crossed to *Df(2L)E55/CyOlacZ* males; all progeny are heterozygous for *Ptp99A*.

Table 4. Summary of results

Guidance decision	Affected in*	Primarily requires
	ISN	
Navigation past 1st branch point	triple	DLAR *or* DPTP69D *or* DPTP99A
Navigation past 2nd branch point	*Dlar Ptp69D*	DLAR *or* DPTP69D
Terminal arbor formation	*Dlar*	DLAR
	SNb	
Defasciculation from ISN at exit junction	triple	DPTP69D *or* DLAR *or* DPTP99A
Entry into VLM field	*Dlar*	Abnormal decision to grow parallel to ISN requires DPTP99A
Pathfinding within VLMs	*Ptp69D Ptp99A*, *Dlar Ptp69D*	DPTP69D
Synaptogenesis	*Dlar*	DLAR

*In each case, the 'minimal' genotype(s) associated with a characteristic phenotype affecting a specific decision is listed. For example, SB truncations are seen in both *Dlar Ptp69D* and the triple, so *Dlar Ptp69D* is listed.

the SN root, often follow normal trajectories even in triple mutants, although SNa is usually thinner and SNc often shorter than in wild-type (Figs 4F, 6B-D).

In addition to motor pathways, the 1D4 antibody also labels three longitudinal axon bundles within the CNS in late stage 16 embryos. These pathways have a normal appearance in all single and double mutants (Fig. 6A-C and data not shown), and are fairly regular in the triple mutant as well (Fig. 6D), suggesting that the three RPTPs are not essential for guidance of most axons within these bundles.

A small percentage of fusion bypass hemisegments in triple mutants have ISN roots that are thinner than normal, suggesting that they might lack SNb axons. Missing SNbs could result from early pathfinding errors by RP growth cones within the CNS, as previously described (Desai et al., 1996). Alternatively, neurons that normally send axons into the motor pathways could be missing or transformed into alternative cell types. We have observed, however, that expression of the Even-skipped transcription factor, which is localized to the aCC, RP2 and U motoneurons, among others, is normal in triple mutants (data not shown). The pattern of PNS cell bodies and axons, as visualized with the 22C10 antibody, is also normal.

DISCUSSION

The neural receptor tyrosine phosphatases DPTP69D, DPTP99A and DLAR are required for guidance of embryonic motor axons (Desai et al., 1996; Krueger et al., 1996). Here we examine the motor axon phenotypes of mutant combinations involving all three of these *Rptp* genes. Our analysis shows that specific RPTPs are required for a number of pathway decisions made by growth cones along the trajectories of the ISN and SNb motor nerves.

The roles of the three RPTPs are specific to particular guidance decisions, because only certain axon pathways are affected in *Rptp* mutants. Among motor axons, the three branches of the ISN root (ISN, SNb, SNd) are strongly affected, while the SN root branches (SNa and SNc) are relatively normal even in mutants lacking DPTP69D, DPTP99A and DLAR (Figs 4F,G, 6). CNS pathways labeled by mAb 1D4 are also not strongly affected in *Rptp* mutants (Fig. 6), and the PNS is completely normal. Finally, SNb axons that bypass their target muscles in the *Rptp* mutants actually extend farther than do normal SNb axons, indicating that outgrowth per se is not inhibited by the loss of RPTP activity.

The relationships among the RPTPs in controlling ISN and SNb axon guidance events are complex and dependent on cellular context. Each of the growth cone pathway decisions made during navigation of these axons to their muscle targets is dependent on a specific combination of RPTPs (summarized in Table 4). Along the ISN pathway two of the RPTPs, DLAR and DPTP99A, function in a cooperative manner. At one of the SNb choice points, however, these two RPTPs oppose each other's activities.

RPTPs and navigation of ISN growth cones past intermediate targets

Our results suggest that ISN pioneer growth cones navigate through sequential recognition of intermediate targets, and that a hierarchy of RPTPs is required for progression of growth cones past these targets (Table 4). If any one of the three RPTPs is expressed, >95% of ISNs grow past the first intermediate target near muscles 3 and 19, but in a triple mutant only about 40% do (Figs 2D, 3). Expression of either DLAR or DPTP69D, but not of DPTP99A, is sufficient to allow >80% of ISNs to grow beyond the second intermediate target near muscles 2 and 10 (Figs 2C, 3). Finally, the terminal arborization at muscles 1 and 9 uniquely requires DLAR (Fig. 2B).

An attractive model to explain these results is that the intermediate targets are analogous to 'guidepost cells' in the grasshopper limb bud, which are recognized by sensory neuron growth cones. Contact between a single filopodium of a sensory neuron and a guidepost cell can reorganize the actin cytoskeleton and steer the entire growth cone toward the guidepost (reviewed by Bentley and O'Connor, 1994). *Drosophila* ISN motoneuron growth cones, including that of the pioneer aCC, have filopodia up to 10 μM in length (Sink and Whitington, 1991), which is sufficient to span the distances between intermediate targets. Pioneer growth cones paused at one target might navigate to the next target through filopodial contact and subsequent reorientation. Sequential recognition of and/or outgrowth to each target would require signaling by specific RPTPs. These roles of RPTPs at the intermediate targets could be instructive, if the targets are labeled by RPTP ligands, or permissive, if other cell-surface molecules are used for target recognition.

One possible permissive model emphasizes the potential roles of RPTPs in regulating fasciculation and adhesion. The fusion bypass and stall phenotypes seen in the *Rptp* mutants resemble those produced by overexpression of the homophilic adhesion molecule Fasciclin II on the motor axons (Lin and Goodman, 1994). This could indicate that one function of the RPTPs might be to reduce adhesion at choice points, permitting growth cones to defasciculate and steer toward the next target. In this model, ISN pioneer growth cones might stick tightly to each intermediate target, and extension into the territory beyond the target would require weakening of this adhesion *via* activation of specific RPTPs.

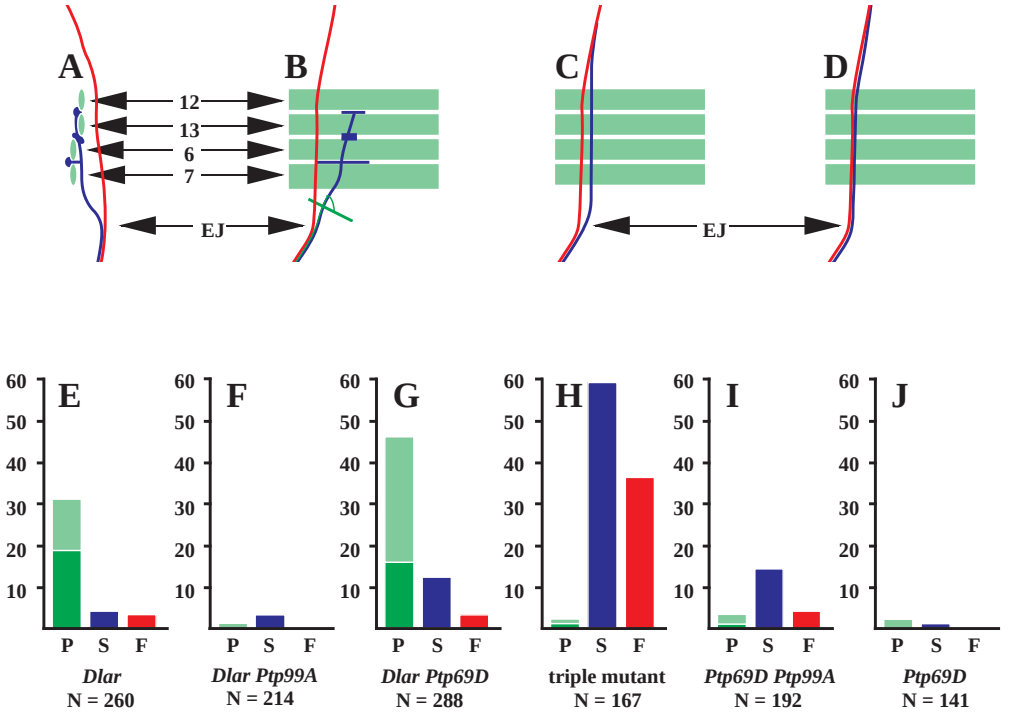

Fig. 5. Schematic diagrams and bar graphs of SNb phenotypes. Four ventrolateral muscles (VLMs; green) are depicted, as are the ISN (red), SNb (blue), and SNd (green). (A) Cross-section of wild-type, showing the exit junction (EJ) and SNb trajectory among the VLMs. (B) Wild-type SNb morphology. The SNb and ISN are indicated on top of the VLMs for clarity, although they actually grow underneath them. (C) Parallel bypass. (D) Fusion bypass. The ordinates of the bar graphs in E-J represent the penetrances (in %) of the various phenotypes. Complete parallel bypass, green bars; partial parallel bypass, light green bars. These categories are combined into one column, labeled P. S: SNb stalls before entry into VLM field (purple bars). F: fusion bypass (red bars). N, number of hemisegments scored. (E) *Dlar*$^{5.5}$/*Dlar*$^{13.2}$. (F) *Dlar*$^{5.5}$/*Dlar*$^{13.2}$; *Df(3R)R3/Ptp99A*^{1}. (G *Dlar*$^{5.5}$/*Dlar*$^{13.2}$; *Ptp69D*^{1}/*Df(3L)8ex25*. (H) *Ptp69D*^{1}*Df(3R)R3/Df(3L)8ex25 Ptp99A*^{1}. (I) *Dlar*$^{5.5}$/*Dlar*$^{13.2}$; *Ptp69D*^{1}*Df(3R)R3/Df(3L)8ex25 Ptp99A*^{1}.

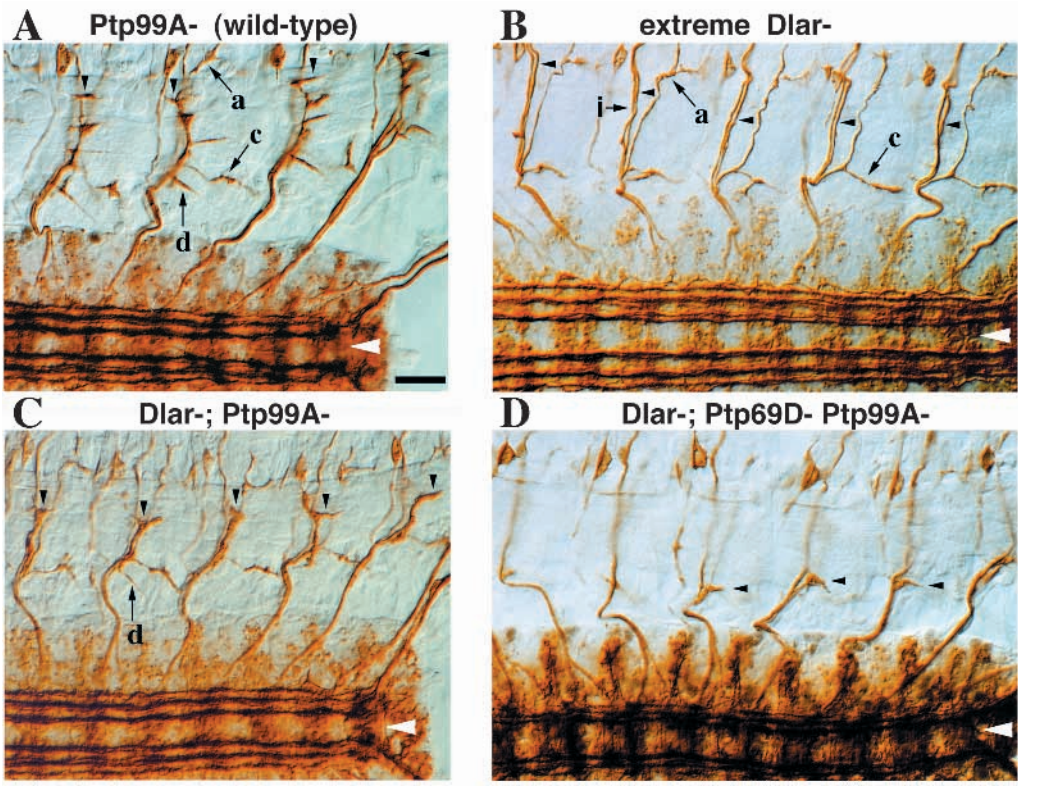

Fig. 6. CNS and SNb pathways in *Rptp* mutants. CNS axon tracts (white arrowhead, CNS midline) and VLMs in late stage 16 mAb 1D4-stained embryos. SNb, small arrowheads; SNa, a; SNc, c; SNd, d; ISN, i. (A) *Ptp99A* (identical to wild-type), A4-A7. Note the regularity of the three longitudinal bundles on each side of the CNS. (B) *Dlar*, A2-A6. The focal plane in this panel is deeper than in the other panels, in order to visualize the bypass axon tracts. The SNbs in this *Df(2L)E55/Dlar*$^{13.2}$ embryo all display the complete parallel bypass (P) phenotype. The SNbs are seen as a distinct tract next to the ISN, under the VLMs (see also Fig. 4E). They appear to rejoin the ISN distal to the VLMs. Note that SNa and SNc appear normal, but that SNd is missing in all five hemisegments. (C) *Dlar, Ptp99A*, A3-A7. Note the characteristic *Dlar*-like morphologies of the SNbs (see Fig. 4D) and the lack of parallel bypass phenotypes. The CNS is almost indistinguishable from wild-type. (D) Triple mutant, A2-A7. Note the dramatic difference between the SNbs in C and D, caused by the loss of *Ptp69D* function. This is a classic example of a synergistic phenotype, because this hypomorphic *Ptp69D* genotype (*Ptp69D*^{1}/*Df(3L)8ex25*) would have a very weak phenotype (10% abnormal SNbs; see Table 2) as a single mutant. In D all hemisegments display fusion bypass or complete stall phenotypes, and the VLMs are uninnervated. The CNS tracts are still regular, but there is more commissural staining than is normal at this stage. Anterior is left. Scale bar, 5 μm.

DLAR and DPTP99A can act together or in opposition to each other at different SNb choice points

Navigation of SNb growth cones to their final synaptic targets on specific VLMs involves a number of distinct pathway decisions that require RPTP signaling. Expression of any one of the three RPTPs is sufficient to allow defasciculation of >95% of SNbs from the common ISN pathway, so they appear to have similar and partially redundant activities at this decision point (Fig. 5). The RPTPs could mediate changes in interaxonal adhesion required for SNb axons to leave the common pathway. In the absence of signaling by any of the three RPTPs, SNb axons would be unable to reduce their adhesion and defasciculate at the exit junction.

In *Dlar* mutants, SNb growth cones sometimes grow alongside the ISN instead of entering the VLM field, producing parallel bypass phenotypes (Krueger et al., 1996; Figs 4E, 5C, 6B). These phenotypes are completely suppressed by the concomitant loss of DPTP99A (Figs 5E,F, 6B,C), suggesting that the parallel bypass decision in *Dlar* embyos is actually due to inappropriate DPTP99A signaling at the muscle entry point. The DPTP99A signal apparently favors the choice of the incorrect pathway that bypasses the VLMs. This signal would normally be turned off or counteracted by DLAR at the muscle entry point, so that when neither RPTP is expressed SNb growth cones enter the muscle field (Table 4). DPTP69D may also have a minor role in counteracting DPTP99A signaling at this choice point, since overexpressing DPTP69D in a *Dlar* background reduces the penetrance of the parallel bypass phenotype (Table 2).

The results described above indicate that DLAR might counteract or inhibit DPTP99A signaling at the muscle entry point. One possible mechanism for inhibition is suggested by the three-dimensional structure of the first catalytic domain of RPTPα (Bilwes et al., 1996). In the crystal, the RPTPα domains are arranged as dimers, and the N-terminal region (‘wedge’) of each monomer appears to block access to the active site of its partner. This arrangement indicates that the dimeric RPTP is likely to be catalytically inactive. Furthermore, earlier work had shown that when the cytoplasmic domain of the RPTP CD45 is forced to dimerize its activity is suppressed (Desai et al., 1993). These data suggest that ligand interaction with an RPTP could either suppress its enzymatic activity by forcing dimerization, or activate it by splitting a preformed dimer.

The wedge region is conserved among the first PTP domains in many RPTPs, including the *Drosophila* neural RPTPs DLAR, DPTP69D, DPTP99A and DPTP10D (Bilwes et al., 1996), suggesting that RPTP heterodimers might also be able to form. Recent results from one of our laboratories show that one such heterodimer, DPTP69D/DPTP10D, does in fact exist in transfected *Drosophila* cells (S. Fashena and K. Z., unpublished results). Thus, the suppression of DPTP99A signaling by DLAR at the VLM entry point could involve the formation of a catalytically inactive DLAR/DPTP99A heterodimer.

We thank Siegfried Roth for the anti-Twist antiserum, Corey Goodman for mAb 1D4, Bill Chia for *Df(3R)KE*, and David Van Vactor and the members of our laboratories for helpful discussions and comments on the manuscript. This work was supported by National Institutes of Health grants NS28182 to K. Z. and GM-53415 to H. S.

Note

For further information on motor axons see http://www.caltech.edu/~zinn/

REFERENCES

Bate, M. (1993). The mesoderm and its derivatives. In *The development of Drosophila melanogaster* (ed. M. Bate and A. Martinez Arias), pp. 1013-1090. Plainview, N.Y.: Cold Spring Harbor Laboratory Press.

Bate, M., Rushton, E. and Currie, D. A. (1991). Cells with persistent *twist* expression are the embryonic precursors of adult muscles in *Drosophila*. *Development* **113,** 79-90.

Beggs, H. E., Soriano, P. and Maness, P. F. (1994). NCAM-dependent neurite outgrowth is inhibited in neurons from fyn-minus mice. *J. Cell Biol.* **127,** 825-833.

Bentley, D. and O’Connor, T. P. (1994). Cytoskeletal events in growth cone steering. *Curr. Opin. Neurobiol.* **4,** 43-48.

Bilwes, A. M., den Hertog, J., Hunter, T. and Noel, J. P. (1996). Structural basis for inhibition of receptor protein-tyrosine phosphatase-α by dimerization. *Nature* **382,** 555-559.

Callahan, C. A., Muralidhar, M. G., Lundgren, S. E., Scully, A. L. and Thomas, J. B. (1995). Control of neuronal pathway selection by a Drosophila receptor protein tyrosine kinase family member. *Nature* **376,** 171-174.

Chant, J. and Stowers, L. (1995). GTPase cascades choreographing cellular behavior: movement, morphogenesis, and more. *Cell* **81,** 1-4.

Chien, C.-B. (1996). PY in the fly: receptor-like tyrosine phosphatases in axonal pathfinding. *Neuron* **16,** 1065-1068.

Debant, A., Serra-Pages, C., Seipel, K., O’Brien, S., Tang, M., Park, S.-H. and Streuli, M. (1996). The multidomain protein Trio binds the LAR transmembrane tyrosine phosphatase, contains a protein kinase domain, and has separate rac-specific and rho-specific guanine nucleotide exchange factor domains. *Proc. Natl. Acad. Sci. USA* **93,** 5466-5471.

Desai, C. J., Gindhart, J. G., Goldstein, L. S. B. and Zinn, K. (1996). Receptor tyrosine phosphatases are required for motor axon guidance in the Drosophila embryo. *Cell* **84,** 599-609.

Desai, D. M., Sap, J., Schlessinger, J. and Weiss, A. (1993). Ligand-mediated negative regulation of a chimeric transmembrane receptor tyrosine phosphatase. *Cell* **73,** 541-554.

Fan, J. and Raper, J. A. (1995). Localized collapsing cues can steer growth cones without inducing their full collapse. *Neuron* **14,** 263-274.

Fashena, S. J. and Zinn, K. (1995). The ins and outs of receptor tyrosine phosphatases. *Curr. Biol.* **5,** 1367-1369.

Goodman, C. S. (1996). Mechanisms and molecules that control growth cone guidance. *Annu. Rev. Neurosci.* **19,** 341-378.

Hamilton, B. A., Ho, A. and Zinn, K. (1995). Targeted mutagenesis and genetic analysis of a *Drosophila* receptor-linked protein tyrosine phosphatase gene. *Roux’s Arch. Dev. Biol.* **204,** 187-192.

Harris, W. A. and Holt, C. E. (1995). From tags to RAGS: chemoaffinity finally has receptors and ligands. *Neuron* **15,** 241-244.

Henkemeyer, M., Orioli, D., Henderson, J. T., Saxton, T. M., Roder, J., Pawson, T. and Klein, R. (1996). Nuk controls pathfinding of commissural axons in the mammalian central nervous system. *Cell* **86,** 35-46.

Ignelzi, M. A., Miller, D. R., Soriano, P. and Maness, P. F. (1994). Impaired neurite outgrowth of src-minus cerebellar nuerons on the cell-adhesion molecule L1. *Neuron* **12,** 873-884.

Keshishian, H., Broadie, K., Chiba, A. and Bate, M. (1996). The *Drosophila* neuromuscular junction – a model system for studying synaptic development and function. *Ann. Rev. Neur.* **19,** 545-575.

Krueger, N. X., Van Vactor, D., Wan, H. I., Gelbart, W. M., Goodman, C. S. and Saito, H. (1996). The transmembrane tyrosine phosphatase DLAR controls motor axon guidance in Drosophila. *Cell* **84,** 611-622.

Lin, D. M. and Goodman, C. S. (1994). Ectopic and increased expression of fasiclin II alters motoneuron growth cone guidance. *Neuron* **13,** 507-523.

Orioli, D., Henkemeyer, M., Lemke, G., Klein, R. and Pawson, T. (1996). Sek4 and Nuk receptors cooperate in guidance of commissural axons and in palate formation. *EMBO J.* **15,** 6035-6049.

Serrapages, C., Kedersha, N. L., Fazikas, L., Medley, Q., Debant, A. and

Streuli, M. (1995). The LAR transmembrane protein-tyrosine phosphatase and a coiled-coil LAR-interacting protein colocalize at focal adhesions. *EMBO J.* **14,** 2827-2838.

Sink, H. and Whitington, P. M. (1991). Location and connectivity of abdominal motoneurons in the embryo and larvae of Drosophila melanogaster. *J. Neurobiol.* **12,** 298-311.

Stoker, A. W., Gehrig, B., Haj, F. and Bay, B.-H. (1995). Axonal localisation of the CAM-like tyrosine phosphatase CRYPα: a signaling molecule of embryonic growth cones. *Development* **121,** 1833-1844.

Tian, S.-S., Tsoulfas, P. and Zinn, K. (1991). Three receptor-linked protein-tyrosine phosphatases are selectively expressed on central nervous system axons in the *Drosophila* embryo. *Cell* **67,** 675-685.

Van Vactor, D., Sink, H., Fambrough, D., Tsoo, R. and Goodman, C. S. (1993). Genes that control neuromuscular specificity in Drosophila. *Cell* **73,** 1137-1153.

(Accepted 24 February 1997)